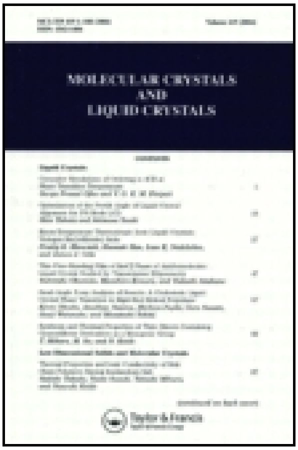

Molecular Crystals and Liquid Crystals
Publication details, including instructions for authors and subscription information:
http://www.tandfonline.com/loi/gmcl20

Microwave Polymer Dispersed Liquid Crystal Loaded Variable Phase Shifter

Toshihisa Kamei [a], Nguyen Quoc Dinh [a] & Yozo Utsumi [a]

[a] Department of Communications Engineering, National Defense Academy, Hashirimizu, Yokosuka, Kanagawa, Japan

Version of record first published: 22 Sep 2010

To cite this article: Toshihisa Kamei, Nguyen Quoc Dinh & Yozo Utsumi (2007): Microwave Polymer Dispersed Liquid Crystal Loaded Variable Phase Shifter, Molecular Crystals and Liquid Crystals, 476:1, 15/[261]-30/[276]

To link to this article: http://dx.doi.org/10.1080/15421400701732589

Mol. Cryst. Liq. Cryst., Vol. 476, pp. 15/[261]–30/[276], 2007
Copyright © Taylor & Francis Group, LLC
ISSN: 1542-1406 print/1563-5287 online
DOI: 10.1080/15421400701732589

Microwave Polymer Dispersed Liquid Crystal Loaded Variable Phase Shifter

Toshihisa Kamei
Nguyen Quoc Dinh
Yozo Utsumi
Department of Communications Engineering, National Defense Academy, Hashirimizu, Yokosuka, Kanagawa, Japan

We discuss a method for the production of microwave polymer dispersed liquid crystal devices and show how to obtain a fine grained uniform fibrous polymer network. With a layer thickness of 50 μm, an applied voltage of 100 V and a polymer concentration of 7 wt%, we show that the decay time can be reduced to about 1/30th that of a plain liquid crystal at the expense of an increase in rise time of about 2.5 times and a deterioration of dielectric birefringence of about 50%. Finally we discuss the results obtained with a prototype polymer dispersed liquid crystal loaded variable phase shifter in the 15 GHz band.

Keywords: delay lines; liquid crystal devices; microstrip resonators; phase shifter

INTRODUCTION

In a liquid crystal device with a microstrip line (MSL) structure, microwave-band insertion losses make it impossible to use an extremely thin liquid crystal layer as in liquid crystal display applications. On the other hand, the decay time of a liquid crystal device increases in proportion to the square of the layer thickness [1], so with a liquid crystal layer thickness of about 100 μm as used in the configuration of most microwave liquid crystal devices, the decay time ends up being about 1000 times greater than the rise time [2].

A part of this research work was supported by the 2004 Hoso Bunka (Broadcasting Culture) Foundation.

Address correspondence to Toshihisa Kamei, Department of Communications Engineering, National Defense Academy, 1-10-20 Hashirimizu, Yokosuka, Kanagawa, 239-8686, Japan. E-mail. kamei@mda.ac.jp

It is thus hoped that a way can be found to substantially reduce the decay time even if this entails a slight increase in rise time and deterioration of the dielectric properties. A promising means of achieving this involves substituting the liquid crystal layer with a so-called polymer dispersed liquid crystal consisting of a polymer dispersed into a nematic liquid crystal at a suitable concentration [3].

In this article, our chief aim is to demonstrate quantitatively how the decay times of devices using polymer dispersed liquid crystals can be improved in order to address a serious issue described in reference [2]—namely the large value of the decay time in plain liquid crystal devices. In order to take direct measurements of the liquid crystal device characteristics in the microwave-band when measuring the response time characteristics and dielectric properties of an MSL structure polymer dispersed liquid crystal devices, we used a microwave resonance method based on an inductive coupled ring resonator that we developed [4,5].

IMPROVING THE DECAY TIME OF POLYMER DISPERSED LIQUID CRYSTAL DEVICES

When a plain liquid crystal is injected between two parallel plates that have been subjected to a rubbing process, the decay time increases in proportion to the square of the liquid crystal layer thickness [1], so once the layer thickness has been set, the device's response time is more or less predetermined. The thickness of the liquid crystal layer for microwave devices is relatively large at about 100 μm, in which case the rubbed substrate surfaces are only able to apply a weak aligning force to the molecular orientation of the liquid crystal so that the rise time is only a few milliseconds while the decay time is much longer at several tens of seconds.

Thus, since the use of a polymer dispersed liquid crystal causes the liquid crystal molecules to be subjected to a strong aligning force from the neighboring polymer interfaces, the same effect is obtained when the liquid crystal layer is made thinner, allowing the decay time to be improved. However, this effect involves trade-offs associated with the disadvantages of increased threshold voltage, lower dielectric birefringence and increased rise time.

$$\tau_r = \eta/\{\varepsilon_0|\Delta\varepsilon'|(\mathrm{E}_0^2 - \mathrm{E}_\mathrm{C}^2)\} \tag{1}$$

$$\tau_d = \eta \mathrm{d}^2/(\pi^2 \mathrm{k}) \tag{2}$$

Here, η is the coefficient of viscosity, E_0 and E_C are the bias electric field and threshold electric field, $\Delta\varepsilon'$ $(= \varepsilon'_{||} - \varepsilon'_{\perp})$ is the dielectric birefringence, and k is the elastic constant.

PRODUCTION OF THE POLYMER DISPERSED LIQUID CRYSTAL MATERIAL

The polymer dispersed liquid crystal was made by mixing a nematic liquid crystal with a photo setting pre-polymer (acryl urethane based, NOA65 made by Norand, refractive index 1.524).

The polymer dispersed liquid crystal was produced by the phase separation method with photopolymerization. An optical test cell was produced to facilitate observation of the formation of a uniform fibrous polymer network, which is desirable in a microwave use. Considering that the polymer dispersed liquid crystal would be applied to microwave-band variable delay lines and the like, the polymer dispersed liquid crystal test cell was produced using the nematic liquid crystals BL006 and BL011 (MERCK), which have relatively large $\Delta\varepsilon'$ in the 20 GHz band, where $\Delta\varepsilon'$ $(=\varepsilon'_{||}-\varepsilon'_{\perp})$ is the dielectric birefringence, and $\varepsilon'_{||}$ is the relative permittivity ε' when the long axis of the liquid crystal molecules is parallel to the high frequency electric field, and $\varepsilon'_{\perp}$ is the relative permittivity ε' when the long axis of the liquid crystal molecules is perpendicular to the high frequency electric field.

Table 1 lists the parameters of these two liquid crystal materials measured in the 20 GHz band and the values shown in the manufacturer's catalog.

The pre-polymer was stirred for several hours while keeping it heated beyond the temperature at which BL006 becomes isotropic (the nematic-isotropic; N-I phase transition temperature = 113°C).

The pre-polymer was mixed in at a ratio of 5 wt%. A test cell was produced by filling the space between two homogeneously aligned ITO (Indium Tin Oxide) glass plates with a uniformly blended mixture. If this filling is performed in the nematic phase then it can give rise to alignment imperfections originating from the orientation caused by flow effect, so as shown in Figure 1(a) the filling is performed with the liquid crystal kept at or above the N-I phase transition temperature and then the cell temperature is gradually reduced.

TABLE 1 Nematic Liquid Crystal (MERCK) Used for Our Measurements

	BL006	BL011
N-I (°C)	+113	+62
$\Delta\varepsilon'$ (1 kHz, 20°C)	+17.3	+16.2
$\Delta\varepsilon'$ (20 GHz, 20°C)	+0.75	+0.6
n_o (ordinary refractive index)	1.53	1.5351
n_e (extraordinary refractive index)	1.816	1.813

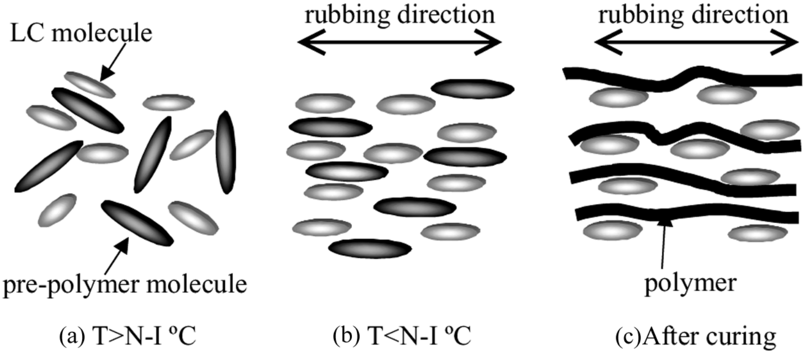

FIGURE 1 Photopolymer phase separation mechanism.

When the temperature falls below the N-I phase transition temperature, the anisotropic nature of the liquid crystal molecules causes them to line up in the rubbing direction. This also affects the pre-polymer molecules, which line up as shown in Figure 1(b). When the pre-polymer is polymerized in this state by irradiating with ultraviolet light, it is possible to obtain a polymer with a uniform orientation as shown in Figure 1(c).

However, it has been reported that the resulting polymer contains bubbles or cavities instead of an organized fibrous structure when the polymer concentration exceeds 20 wt% [6].

Figure 2 shows the optical observation system used for the test cell. This system uses a polarizing microscope incorporating a polarizer and an analyzer. A bias voltage was provided by amplifying a 1 kHz pulse train produced by a function generator. The transparent axes of the polarizer and analyzer were arranged in an orthogonal crossed Nichols configuration.

With no voltage applied, a bright image is obtained for two reasons: (i) the polarization plane rotates due to the uniaxial anisotropic characteristics of the liquid crystal molecules because the optical axis of the molecules is not parallel to the direction in which the light propagates, and (ii) the transmitted light is scattered in the polymer dispersed liquid crystal due to the difference in refractive index between the liquid crystal ($n_e = 1.816$, permittivity close to the $\varepsilon'_\perp$ state) and the polymer (1.524).

Here, the reason why the resulting permittivity is "close to" the $\varepsilon'_\perp$ state is thought to be because—due to the three-dimensional structure of the polymer—some of the liquid crystal molecules restrained by the polymer subtend an angle to the substrate even when no voltage is applied, so that the permittivity is not exactly equal to $\varepsilon'_\perp$.

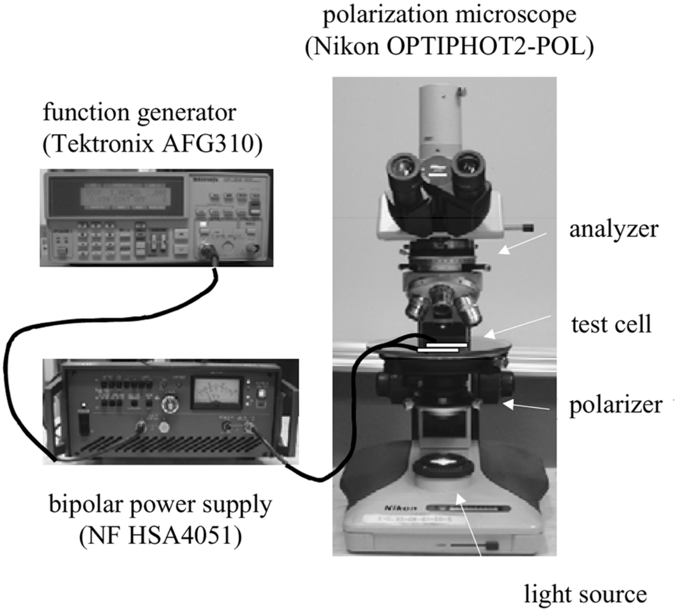

FIGURE 2 Experimental setup for a polymer dispersed liquid crystal test cell.

When a voltage is applied to this cell, the incident plane-polarized light passes straight through the cell and a dark image is obtained for two reasons: (i) the optical axis matches the light propagation direction, so the polarization plane does not rotate, and (ii) the refractive indices of the liquid crystal and polymer become more or less equal ($n_0 = 1.53$, permittivity in the $\varepsilon'_{||}$ state) so that the transmitted light is not scattered.

Figure 3 shows a photograph of a polymer dispersed liquid crystal with no applied voltage. This was produced by mixing 5 wt% NOA65 into BL006 at or above the N-I phase transition temperature (113°C) and allowing it to polymerize at room temperature. Whereas Figure 1 showed the ideal state where the pre-polymer is uniformly dispersed in the liquid crystal and is affected by the alignment of the liquid crystal molecules when it undergoes photopolymerization to yield a neatly ordered polymer network, the photograph in Figure 3 reveals a random formation with a schlieren texture [7], showing that the liquid crystal is also randomly oriented.

To investigate the causes of this, we turned our attention to the temperature during the polymer dispersed liquid crystal mixing.

When the nematic liquid crystal BL011 (MERCK), which has a low phase transition temperature, was mixed with NOA65 at a polymer

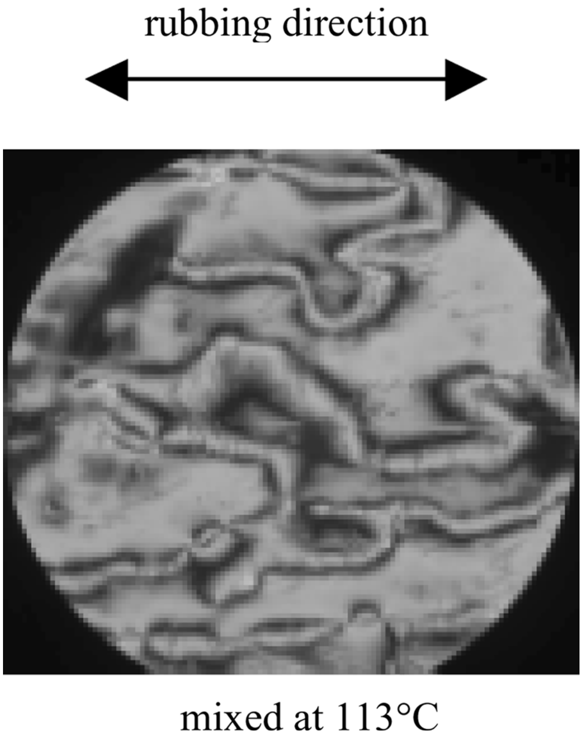

FIGURE 3 A polymer dispersed liquid crystal made by mixing 5 wt% NOA65 into BL006.

concentration of 5 wt% and at the N-I phase transition temperature of BL006 (113°C), we observed schlieren texture and non-uniformities similar to those obtained with BL006, as shown in Figure 4(a). Next, when the same material was mixed at the N-I phase transition temperature of BL011 (62°C), we found that we could obtain a fine-grained uniform fibrous polymer network as shown in Figure 4(b).

These results clearly show that NOA65 deteriorates at high temperatures, preventing it from mixing uniformly with the liquid crystal.

We therefore decided to use the nematic liquid crystal BL011 in the subsequent experiments because it has a lower N-I phase transition temperature, even though its $\Delta\varepsilon'$ is slightly less than that of BL006 (about 0.6, compared with about 0.75 for BL006).

Using the nematic liquid crystal BL011 and the pre-polymer NOA65, we prepared samples with a variety of polymer concentrations and cell thicknesses. Figure 5 shows the appearance under the microscope of polymer dispersed liquid crystals with a pre-polymer concentration of 5 wt% and cell thicknesses (d) of 7.5 and 50 µm. A uniform polymer network was observed at both cell thicknesses.

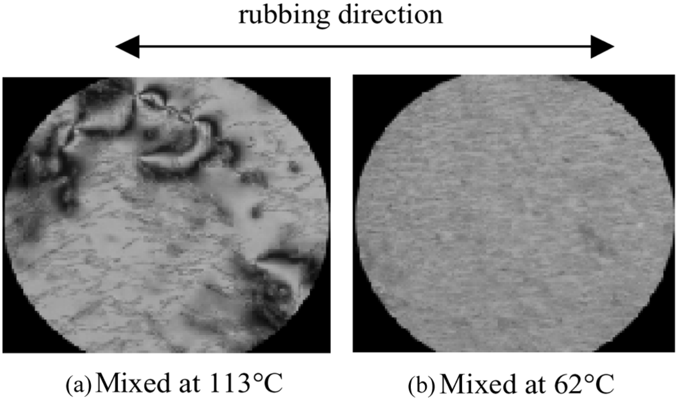

FIGURE 4 Polymer dispersed liquid crystals made by mixing 5 wt% NOA65 into BL011.

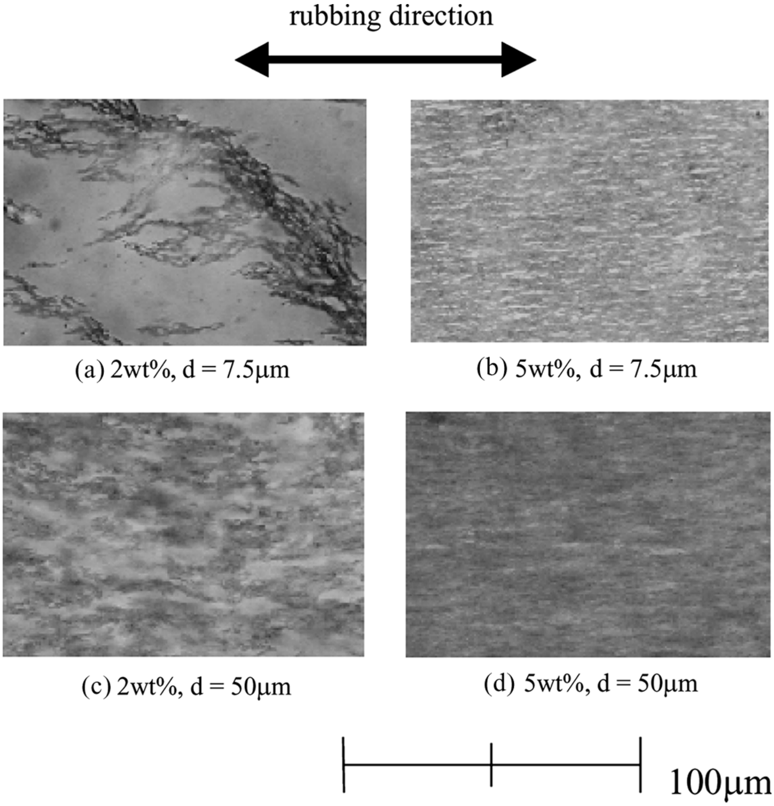

FIGURE 5 Polymer dispersed liquid crystals made by mixing BL011 with 2 wt% and 5 wt% of NOA65.

Figure 5 also shows the appearance of polymer dispersed liquid crystals with a polymer concentration of 2 wt%. In this case, the uniformity of the fibrous polymer network is slightly worse, and it appears that the orientation of the liquid crystal molecules is less strongly restrained by the polymer. We also performed experiments with a polymer concentration of 1 wt%, but there appeared to be no polymer networks in the resulting structures and it is thus thought that 2 wt% is the lower limit for the formation of a uniform polymer network with this liquid crystal/pre-polymer combination. Thus, the mixture was prepared with between 2% and 14% by weight of pre-polymer.

PERMITTIVITIES AND DIELECTRIC BIREFRINGENCE

The permittivities and dielectric birefringence ($\Delta\varepsilon'$) of the polymer dispersed liquid crystal were measured by a method involving the use of the ring resonator [2]. Here, the cell thickness was set to 50 μm.

Figure 6 shows the permittivities and $\Delta\varepsilon'$ of the polymer dispersed liquid crystal. For these measurements we used the resonant peak in the vicinity of 20 GHz, and the value of $\varepsilon'_{||}$ was measured by applying a 1 kHz, 100 V rectangular voltages. In this figure, the symbols ●, ▲ and ■ at 0 wt% indicate the liquid crystal material's own dielectric properties as determined using the cutback method described in reference [4].

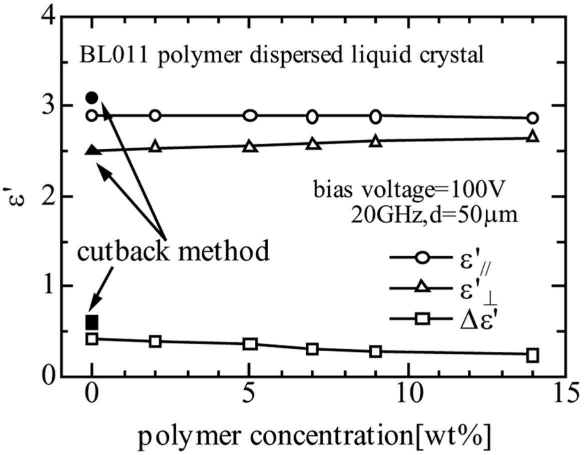

FIGURE 6 Polymer concentration dependence of $\varepsilon'_{||}$, $\varepsilon'_{\perp}$, and $\Delta\varepsilon'$.

The value of $\varepsilon'_{\perp}$ at a polymer concentration of 0% (plain liquid crystal) is the same as the value obtained with the cutback method in an MSL structure used here, but the value of $\varepsilon'_{||}$ was smaller than the value obtained with the cutback method due to the effects of incomplete alignment as discussed in references [4] and [5]. As the polymer concentration increases, the value of $\varepsilon'_{||}$ gradually decreases and the value of $\varepsilon'_{\perp}$ increases so that $\Delta\varepsilon'$ $(= \varepsilon'_{||} - \varepsilon'_{\perp})$ becomes smaller.

By comparing the reduction of $\varepsilon'_{||}$ and the increase of $\varepsilon'_{\perp}$ that occur as the polymer concentration increases, it can be said that the increase of $\varepsilon'_{\perp}$ is larger and thus the reduction of $\Delta\varepsilon'$ is dominated by the increase of $\varepsilon'_{\perp}$. The value of $\varepsilon'_{\perp}$ is thought to increase because the liquid crystal molecules are affected by the polymer interfaces (which are configured in three dimensions), so that the liquid crystal molecules have some degree of tilt when there is no applied voltage. On the other hand, the value of $\varepsilon'_{||}$ is thought to decrease slightly due to the polymer's permittivity of 2.3 being slightly smaller than the value of $\varepsilon'_{||}$, so that increasing the polymer concentration causes the value of $\varepsilon'_{||}$ to fall below the value for the liquid crystal. The value of $\Delta\varepsilon'$ was 0.4 at a polymer concentration of 0 wt%, decreasing to $\Delta\varepsilon' = 0.33$ at 5 wt%, $\Delta\varepsilon' = 0.31$ at 7 wt%, $\Delta\varepsilon' = 0.28$ at 9 wt%, $\Delta\varepsilon' = 0.23$ at 14 wt%.

Thus the dispersal of a polymer into the liquid crystal can improve τ_d at the expense of a reduced value of $\Delta\varepsilon'$.

VARIATION OF RESPONSE TIME WITH POLYMER CONCENTRATION

Using the microwave resonance method [2], we measured the response time characteristics with respect to changes in the polymer concentration in the microwave-band with a fixed layer thickness of 50 μm and a bias voltage of 100 V. The measurement results are shown in Figure 7. In these results, the decay time τ_d was about 20 s for the plain liquid crystal, decreasing to 1.6 s with the addition of 5 wt% polymer, approximately 700 ms at 7 wt%, approximately 650 ms at 9 wt% and approximately 500 ms at 14 wt%.

The rise time of the plain liquid crystal was about 10 ms, but this increased to 22 ms with the addition of 5 wt% polymer, 25 ms at 7 wt%, about 28 ms at 9 wt%, and about 36 ms at 14 wt%, which is an acceptable range. Thus as the polymer concentration increases, τ_r becomes larger and τ_d becomes smaller.

This is because a higher polymer concentration results in a denser polymer network so that the liquid crystal molecules drifting through this network are subjected to a stronger aligning force from the

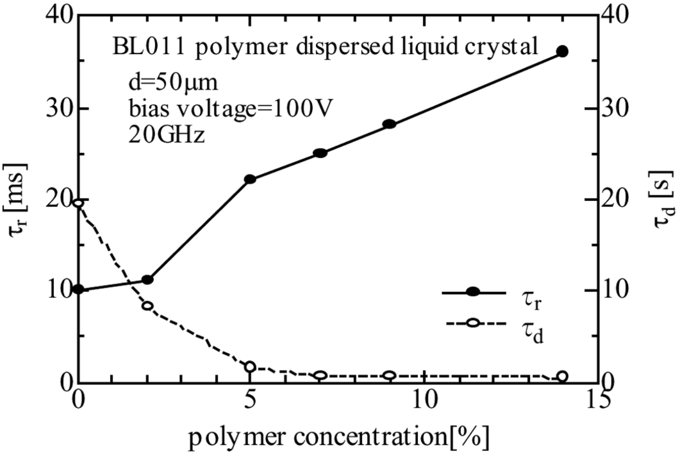

FIGURE 7 Response time (τ_r, τ_d) performances of polymer dispersed liquid crystal for polymer concentration change.

neighboring polymer interfaces. Thus by using a polymer dispersed liquid crystal it is possible to greatly improve τ_d but at the expense of an increase in τ_r.

VARIATION OF POLYMER DISPERSED LIQUID CRYSTAL RESPONSE TIME WITH LAYER THICKNESS

We measured the values of τ_d and τ_r using the microwave resonance method [2] under constant conditions of a polymer concentration of 5 wt% and 9 wt% and an applied electric field of 1.8×10^6 V/m.

Figures 8 and 9 show the results of measuring τ_d and τ_r respectively in polymer dispersed liquid crystal layer thicknesses of 20, 50, 75 and 100 μm.

In Figure 8 the relationship as shown in Equation (2) breaks down due to the aligning force of the polymer, and instead τ_d rises with increasing d at a much slower rate than the square of d.

We obtained a value of $\tau_d = 800$ ms at $d = 20$ μm, increasing to 1.6 s at 50 μm, 2.2 s at 75 μm, and 2.9 s at 100 μm for 5 wt%, and a value of $\tau_d = 650$ ms, 1.25 s, 2.5 s at d = 20, 50, 100 μm respectively for 9 wt%, but this is much better than the 20 s at $d = 50$ μm with the plain liquid crystal.

With regard to τ_r, it does not vary with d in a plain liquid crystal as shown in Equation (1), but in a polymer dispersed liquid crystal it

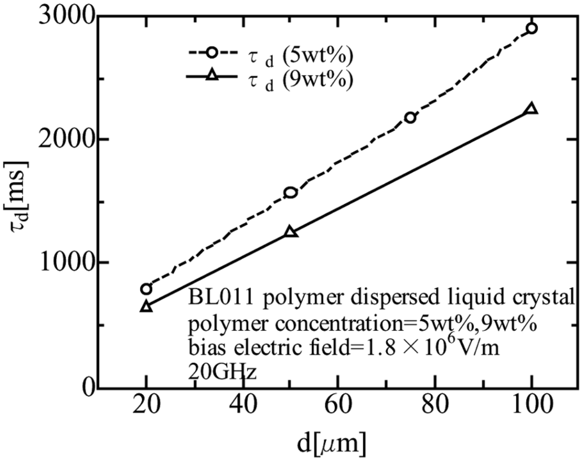

FIGURE 8 Response time (τ_d) performances of polymer dispersed liquid crystal for layer thickness changes.

decreases as d increases as shown in Figure 9. The value of τ_r was 37 ms at $d = 20\,\mu m$, decreasing to 24 ms at 50 μm, 21 ms at 75 μm, and 19 ms at 100 μm for 5 wt%, and $\tau_r = 224$ ms, 26 ms, 25 ms at $d = 20$, 50, 100 μm respectively for 9 wt%.

If the liquid crystal molecules in the polymer dispersed liquid crystal layer are in contact with the polymer network and are greatly

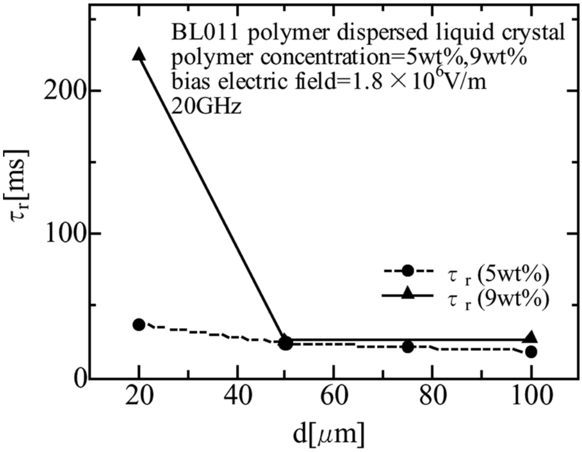

FIGURE 9 Response time (τ_r) performances of polymer dispersed liquid crystal for layer thickness changes.

restrained by it, then it also follows that liquid crystal molecules existing separately from the polymer network are hardly affected at all. Also, the polymer network itself is not uniform but is denser in some parts and sparser in others. Accordingly, it is thought that some of the liquid crystal molecules are strongly affected by the polymer network, while others are less affected. However, since τ_r is defined as the time taken for $\Delta\varepsilon'$ to change by 90% of its saturated value, it is governed by molecules that are strongly affected by the restraining action of the polymer network. When the thickness d of the polymer dispersed liquid crystal layer is small, it is thought that the formation of the polymer network is more susceptible to the effects of the rubbing direction compared with cases where d is large, and that a network is formed parallel to the rubbing plane, and hence it is thought that there are a relatively large number of molecules constrained in a direction parallel to the rubbing plane.

This is thought to be a reason why τ_r increases as d becomes smaller, as shown in Figure 9.

On the other hand, the reason why τ_d becomes larger as d increases as shown in Figure 8 is thought to be because a larger value of d means that the polymer network forms as a mixture with some parts that are parallel to the rubbing plane and others that have a perpendicular orientation, so that the restraining force in the direction parallel to the rubbing plane becomes relatively small.

A POLYMER DISPERSED LIQUID CRYSTAL LOADED VARIABLE PHASE SHIFTER

Figure 10 shows the structure of a prototype 15 GHz band polymer dispersed liquid crystal loaded variable phase shifter. This device has a polymer dispersed liquid crystal layer thickness of $d = 100\,\mu\text{m}$, an MSL-type meander line length of $l = 165\,\text{mm}$, and a line width of $w = 100\,\mu\text{m}$. To control the phase, this variable phase shifter is subjected to a DC bias field of 0–160 V. This polymer dispersed liquid crystal was fabricated by mixing a concentration of 9 wt% and 14 wt% pre-polymer NOA65 into the nematic liquid crystal BL011. Figure 11 shows the photograph of the prototype PDLC loaded phase shifter.

Figure 12 shows the variable phase vs. bias voltage characteristics of the variable phase shifter at 9 wt% and 14 wt%, and Figure 13 shows the response time characteristics of 9 wt% PDLC at each bias voltage.

Figure 12 shows the results of measuring the variable phase as the bias voltage is varied from 0 V to 160 V. A variable phase range of 130°

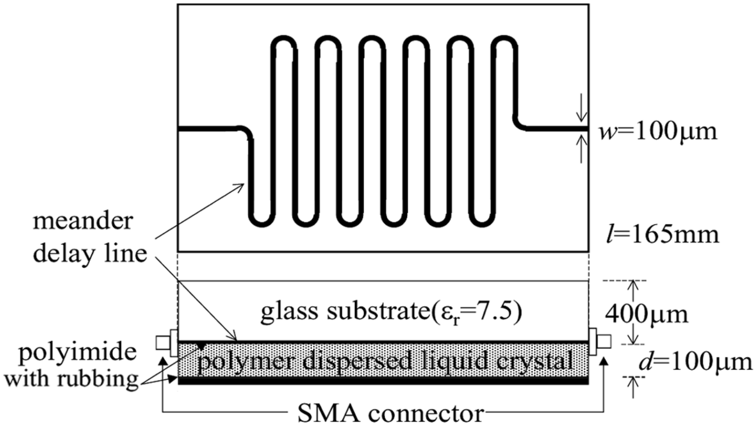

FIGURE 10 Structure of a polymer dispersed liquid crystal loaded variable phase shifter.

was achieved. A phase of 130° was obtained at bias voltages of 150 V or above, and we decided to check the validity of this value from the values of $\varepsilon'_{||}$ and $\varepsilon'_{\perp}$ shown in Figure 6. The results shown in Figure 6 were measured at 20 GHz, which is different from the frequency of 15 GHz in Figure 12, but it can be assumed that the permittivity of the liquid crystal remains equal across this range of frequencies [4].

From Figure 6 we find that $\varepsilon'_{||} = 2.89$, $\varepsilon'_{\perp} = 2.61$, and $\Delta\varepsilon' = 0.28$. In an MSL structures shown in Figure 10, the effective permittivity is smaller than this value due to the effects of the air layer above an MSL.

If $\varepsilon'_{||\mathrm{eff},}$ $\varepsilon'_{\perp\mathrm{eff}}$, and $\Delta\varepsilon'_{\mathrm{eff}}$ are the effective values of $\varepsilon'_{||}$, $\varepsilon'_{\perp}$, and $\Delta\varepsilon'$, then the results of electromagnetic simulation show that these values degrade to $\varepsilon'_{||\mathrm{eff}} = 2.07, \varepsilon'_{\perp\mathrm{eff}} = 1.95$ and $\Delta\varepsilon'_{\mathrm{eff}} = 0.12$. If λ_o is the

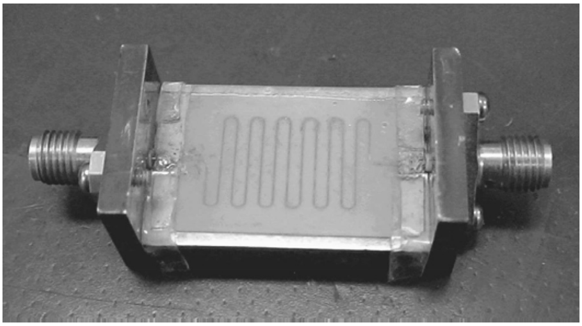

FIGURE 11 Photograph of PDLC loaded phase shifter.

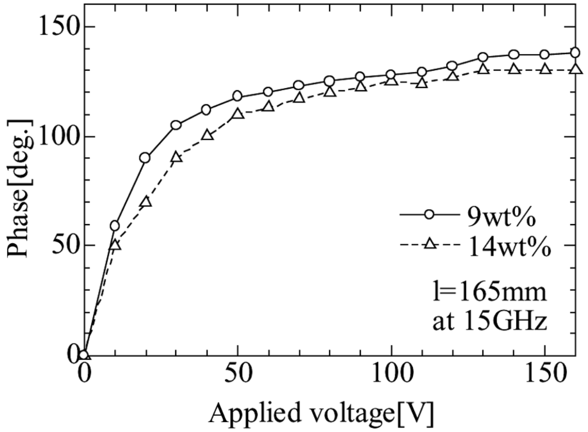

FIGURE 12 Variable phase vs. bias voltage characteristics of the variable phase shifter.

free-space wavelength at the measurement frequency and l is the length of the meander delay line in Figure 10, then the variable phase θ can be expressed by Eq. (3) as follows.

$$\theta = \frac{360\,l}{\lambda_0}\left(\sqrt{\varepsilon_{||\mathrm{eff}}} - \sqrt{\varepsilon_{\perp\mathrm{eff}}}\right) \quad [\text{degree}] \tag{3}$$

By substituting the values $l = 165\,\mathrm{mm}$ and $\lambda_0 = 20\,\mathrm{mm}$ (15 GHz) into this equation, we obtain $\theta = 126^\circ$, which is fairly close to the experimental value of $\theta = 138^\circ$ of 9 wt%PDLC and 130° of 14 wt%PDLC. However, since the results in Figure 6 were obtained with a bias voltage of 100 V and a thickness of $d = 50\,\mu\mathrm{m}$, and $\mathrm{d} = 100\mu\mathrm{m}$ in Figure 12, we selected the value of 130° obtained at a bias voltage of 150 V or above as the comparative phase quantity.

In Figure 13, τ_r and τ_d both become smaller as the bias voltage increases. At a bias voltage of 160 V, they reach values of $\tau_\mathrm{r} = 29\,\mathrm{ms}$ and $\tau_\mathrm{d} = 2.2\,\mathrm{s}$, which are roughly the same as the values of τ_r (the 9 wt% value shown in Figure 9) and τ_d (the 9 wt% value shown in Figure 8) obtained by the microwave resonance method. Figure 13 also shows that τ_r becomes smaller as the bias voltage increases, in agreement with Eq. (1), but the fact that τ_d also becomes smaller needs further investigation.

τ_d is defined as the time taken for the permittivity to decrease by 90% of its saturated value when the permittivity changes from $\varepsilon'_{||}$ to $\varepsilon'_{\perp}$ from the instant the voltage is turned off. With a bias voltage of

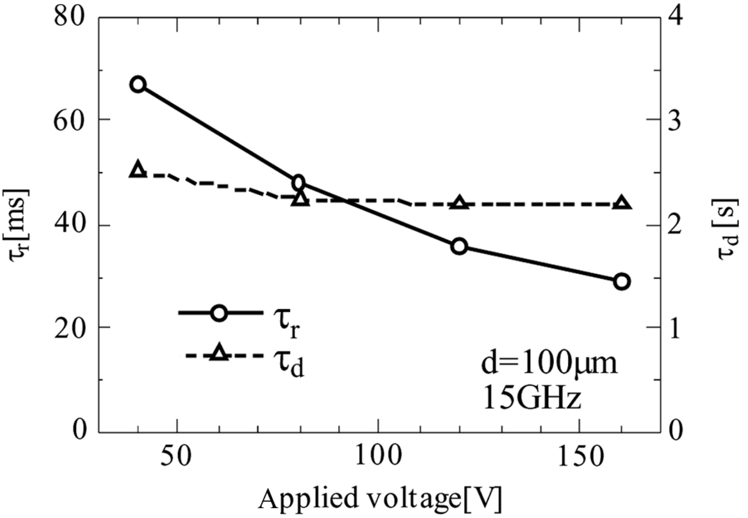

FIGURE 13 Response time (τ_r, τ_d) vs. DC bias voltage characteristics of the variable phase shifter.

160 V, the liquid crystal molecules stand completely perpendicular to the substrate surfaces, but at 40 V they stand at a smaller non-perpendicular angle. Accordingly, if the fall time is measured after turning off a bias voltage of 40 V, then it should be possible to make a more strict assessment of the time taken for the liquid crystal molecules to become parallel to the substrate surfaces compared with a bias voltage of 160 V, and as mentioned in section VI, there may also be problems in the definition of response times due to increases of τ_d caused by regions of polymer that are not completely parallel to the substrate surfaces.

CONCLUSION

We have proposed using a polymer dispersed liquid crystal to improve the response time characteristics of microwave- band liquid crystal adaptive devices.

Concerning with the production method for microwave polymer dispersed liquid crystal devices, we showed the guidelines for the selection of liquid crystal material related to the N-1 phase temperature and the polymer concentration.

Also, using a microwave resonance method that we proposed, we have measured how the dielectric properties and response time characteristics change with the concentration of dispersed polymer in the polymer dispersed liquid crystal and we have clarified the quantitative relationship between them.

As a result, we found that the optimal concentration lies in the range of approximately 7–14 wt%, and that the decay time can be reduced to about 1/30th that of a conventional liquid crystal device. However, the improvement of decay time that results from using a polymer dispersed liquid crystal comes at the expense of an increased rise time and additional insertion loss based on reduction of the dielectric birefringence under conditions where a fixed phase quantity is obtained in the development of devices such as variable delay lines operating in the microwave-band.

We have quantitatively illustrated the trade-off relationship between the improved decay time and these demerits.

Furthermore, although conventional wisdom dictates that τ_r and τ_d are both independent of the polymer dispersed liquid crystal layer thickness, we have found that τ_d increases and τ_r decreases as the polymer dispersed liquid crystal layer becomes thicker at the relatively low polymer concentrations of 2–14 wt% dealt with in this article, and we have quantitatively clarified this layer thickness dependence.

Based on measurements of $\varepsilon'_{||}$, $\varepsilon'_{\perp}$, τ_r and τ_d in polymer dispersed liquid crystals made using the microwave resonance method, we have produced a prototype 15 GHz microstrip meander line polymer dispersed liquid crystal loaded variable phase shifter, and by comparing the variable phase and response time with basic experimental data obtained by the microwave resonance method in this article, we have verified the validity of these values.

REFERENCES

[1] Jakeman, E. & Raynes, E. P. (1972). *Phys. Lett. A*, *39*, 69.
[2] Utsumi, Y., Kamei, T., Naito, R., & Saito, K. (2005). *Mol. Cryst. Liq. Cryst.*, *434*, 337.
[3] Fujikake, H., Kuki, T., Nomoto, T., Tsuchiya, Y., & Utsumi, Y. (2001). *J. Appl. Phys.*, *89*, 5295.
[4] Utsumi, Y. & Kamei, T. *Mol. Cryst. Liq. Cryst.*, *409*, 355.
[5] Utsumi, Y., Kamei, T., & Naito, R. (2003). *Electron Lett.*, *39*, 849.
[6] Fujikake, H., Aida, T., Takizawa, K., Kikuchi, H., Kawakita, M., & Yonai, J. (2000). *IEICE Trans. C*, *J83-C*, 165.
[7] Demus, D. & Richter, L. (1978). *Textures of Liquid Crystals*, Weinheim, Germany: Verlag Chemie.